Energy Conversion and Management 291 (2023) 117257

Contents lists available at ScienceDirect

Energy Conversion and Management

journal homepage: www.elsevier.com/locate/enconman

System-driven design of flexible nuclear power plant configurations with thermal energy storage

Marko Aunedi [a,*], Abdullah A. Al Kindi [b], Antonio M. Pantaleo [b,c], Christos N. Markides [b], Goran Strbac [a]

[a] Department of Electrical and Electronic Engineering, Imperial College London, London SW7 2AZ, UK
[b] Clean Energy Processes (CEP) Laboratory, Department of Chemical Engineering, Imperial College London, London SW7 2AZ, UK
[c] Department of Agro-environmental Sciences, University of Bari, 70121 Bari, Italy

ARTICLE INFO

Keywords:
Flexible nuclear
Nuclear power
Power system flexibility
System-driven design
Thermal energy storage

ABSTRACT

Nuclear power plants are expected to make an important contribution to the decarbonisation of electricity supply alongside variable renewable generation, especially if their operational flexibility is enhanced by coupling them with thermal energy storage. This paper presents a system modelling approach to identifying configurations of flexible nuclear plants that minimise the investment and operation costs in a decarbonised energy system, effectively proposing a system-driven design of flexible nuclear technology. Case studies presented in the paper explore the impact of system features on plant configuration choices. The results suggest that cost-efficient flexible nuclear configurations should adapt to the system they are located in. In the main low-carbon scenarios and assuming standard-size nuclear power plants (1,610 MW_{el}), the lowest-cost system configuration included around 500 MW_{el} of additional secondary generation capacity coupled to the nuclear power plants, with 4.5 GWh_{th} of thermal storage capacity and a discharging duration of 2.2 h. Net system benefits per unit of flexible nuclear generation for the main scenarios were quantified at £29-33 m/yr for a wind-dominated system and £19-20 m/yr for a solar-dominated system.

1. Introduction

Over the past two decades, there have been significant efforts to achieve the ambitious energy decarbonisation targets by expanding low- or zero-emission energy sources such as renewables and nuclear energy. Nuclear power plays an important role in achieving these targets, not only by reducing the emissions but also by being a reliable and non-intermittent source of power compared to renewable sources such as wind and solar [1]. However, nuclear power is not very economically attractive due to its high capital costs compared to lower-cost renewable options, long construction times, and limited load following capabilities [2].

Nevertheless, nuclear power will be essential for ensuring energy security in electricity systems with high shares of variable renewable sources. Its importance has come into focus in light of the recent Ukraine-Russia conflict, with several European countries recognising the need to secure domestic energy production with reduced dependence on energy imports. For example, France, which relies heavily on nuclear power that provides 70 % of its electricity, announced in early 2022 plans to construct six new nuclear reactors [3]. France also considers building a further eight reactors in the future to secure its energy supply and reduce reliance on other countries [3]. Security of supply represents one of the main reasons why the United Kingdom (UK) is also considering future investments in nuclear power [4], in addition to the need to achieve the target of net-zero greenhouse gas emissions by 2050 under the Climate Change Act [5,6]. Future UK government investment plans envisage expanding current nuclear capacity by four times in 2050, from 6 to 24 GW_{el} [7].

Nuclear power plants are commonly operated as baseload units due to their technical characteristics and economic properties, characterised by very high capital cost but very low operating cost. Yet, it is of great interest to investigate the potential of enhancing the flexibility of nuclear power plants in order to both compete with renewables in generating zero-carbon electricity while also supplying peak demand and providing flexible system services. Benefits of upgrading flexibility in energy systems with high shares of renewables have been investigated comprehensively by Strbac et al. [8], where various flexible solutions such as energy storage, demand-side response (DSR), network expansion, flexible generation technologies and sector coupling have been

* Corresponding author.
E-mail address: m.aunedi@imperial.ac.uk (M. Aunedi).

https://doi.org/10.1016/j.enconman.2023.117257

Available online 9 June 2023

Nomenclature

Subscripts/superscripts and acronyms

AGR	advanced gas-cooled reactor
BECCS	bioenergy with carbon capture and storage
BESS	battery energy storage system
bs	battery storage
CAPEX	capital (investment) cost
CCGT	combined cycle gas turbine
ch	charging
dch	discharging
DHN	district heat network
DSR	demand-side response
el	electricity supply system
el–	demand shifted away from given hour
el+	demand shifted towards given hour
elH2	electrolysis
EV	electric vehicle
ex	existing capacity
ext	external (demand)
fn, FN	flexible nuclear
gen	generation
HP	heat pump
hs	hydrogen storage
imp	hydrogen imports
IR	interest rate
LAES	liquid air energy storage
LCOE	levelised cost of electricity
max	maximum
min	minimum
new	new capacity
OCGT	open cycle gas turbine
OPEX	operating cost
PCM	phase change material
PSRC	primary steam Rankine cycle
PV	photovoltaics
ref	methane reforming
RES	renewable energy sources
SG	steam generator
SOC	state of charge
SSRC	secondary steam Rankine cycle
TES	thermal energy storage
UK	United Kingdom
WeSIM	whole-electricity system investment model

Greek symbols

Δ	duration of unit interval (hours)
Φ	annual emission limit (tCO_2/yr)
Ω	maximum annual utilisation factor
α	no-load heat rate (MWh_{th}/hr)
β	incremental heat rate (MW_{th}/MW_{el})
γ	share of demand that can be shifted
δ	volume of demand shifted (MW_{el})
$\in$	carbon emissions per unit of fuel (tCO_2/MWh)
η	efficiency (%)
μ	newly added capacity (MW)
ξ	hydrogen production or consumption (MW_{H2})
π	per-unit cost (£/MW/yr)
τ	storage duration (hours)
φ	system cost component (£)
ψ	efficiency of demand shifting
ω	relative minimum output level

Symbols

A	variable operation cost coefficient (non-fuel) (£/MWh)
D	electricity demand before DSR (MW_{el})
E	number of electrolyser assets
F	number of flexible nuclear assets
G	number of power generation assets
H	number of hydrogen storage assets
HG	set of H_2-fuelled electricity generation technologies
I	number of hydrogen import sources
K	number of demand segments
L	specific consumption per unit of H_2 output (MW/MW_{H2})
M	maximum capacity (MW)
R	number of methane reformer assets
RG	set of renewable electricity generation technologies
S	number of battery storage assets
T	number of unit time intervals
TG	set of thermal electricity generation technologies
U	number of hydrogen storage assets
Y	cost of fuel (£/MWh)
a	normalised availability factor for RES
c	operating cost function (£)
d	electricity demand after DSR (MW_{el})
e	electrolyser asset index
f	flexible nuclear asset index
g	generation asset index
h	heat output/input (MW_{th})
i	hydrogen import source index
k	demand segment index
n	number of units in operation
p	power output (MW_{el})
q	energy content of energy storage (MWh)
r	methane reformer asset index
s	battery storage asset index
t	time interval (hours)
u	hydrogen storage asset index
w	output curtailment (MW_{el})
z	total system cost (£)

identified as beneficial for delivering cost-efficient integration of renewables. Studies for the UK electricity system have clearly shown that flexibility becomes increasingly important as carbon emissions targets for the electricity sector are reduced to achieve net-zero carbon or net-negative carbon electricity supply [9].

Other studies have more specifically addressed the commercial benefits of enhancing the flexibility of nuclear power plants in low-carbon energy systems. A study by Jenkins et al. [10] concluded that flexible nuclear operation could increase the revenues of nuclear power plants by 2–5 % compared to conventional baseload units. The increase of revenues is primarily attributed to the ability of avoiding negative day-ahead electricity prices and supplying day-ahead reserves. Furthermore, Denholm et al. [11] assessed the impact of coupling thermal energy storage (TES) systems with nuclear reactors. The use of TES systems was recommended in the study to attain lower levelised cost of electricity (LCOE) and higher capacity factors, particularly in electricity systems where nuclear is competing with variable renewables such as solar and wind power. Curtis et al. [12] studied the comparative advantages and drawbacks of various options for coupling TES with nuclear generation units, in particular with respect to discharging TES into the primary Rankine cycle against discharging into a secondary cycle.

Coupling nuclear reactors with TES systems and secondary power generation units for greater flexibility and higher revenues was investigated in detail by several authors. For example, Carlson et al. [13] performed a thermodynamic analysis of combining a pressurised water reactor (PWR) with a TES system and steam Rankine cycle-based power generators. In their study, four different configurations based on the location of the TES system (i.e., the charging/discharging point of TES system) were proposed. The study concluded that the configuration where the TES tanks are charged by steam extracted before the high-pressure turbines and then discharged using the optimised secondary power cycles gives the best thermodynamic performance. It was also found that this option increases the capacity factor by 15 % compared to operating the unit in baseload regime. Other studies by the same authors suggested that the approach to integrating TES into the nuclear power cycle would have an impact on the achievable capacity factors and the flexibility that could be provided [14,15].

Another study by Li et al. [16] proposed the integration of nuclear power plant with a cryogenic-based energy storage technology and secondary power generators. The investigated configuration showed the potential of providing a peak power output that is 2.7 times greater than the baseload power output of 250 MW_{el}. Several other studies considered nuclear reactors coupled with different types of TES systems for enhanced flexibility. These TES systems included geothermal heat storage [17], molten-salt tanks [18], hot rock storage [19], cryogenic air [20] and compressed carbon dioxide energy storage systems [21]. These studies demonstrated the benefits arising from enhanced flexibility when integrating nuclear reactors with TES and secondary power cycle systems. Jiang et al. [22] proposed an amine-based TES based on a thermally reversible amine-CO_2 reaction that can store low-grade heat and deliver high-grade heat with a reported efficiency of over 70 %.

Duan et al. [23] performed a stylised least-cost analysis of flexible nuclear power in decarbonised electricity systems while considering wind and solar resources worldwide. The study investigated the role of conventional and flexible nuclear power in 42 country-level electricity systems with carbon emission reduction constraints ranging from 50 % to 100 %. This study looked at different investment cost levels for nuclear plants and different wind power capacity factors. It was found that wind and solar generation provide the bulk of electricity in most of the studied regions with moderate carbon emission reduction targets (i.e., less than 80 %) as this still allows some room for fossil-fuel generation sources in the electricity mix. However, the need for flexible nuclear, enabled through integration with TES, becomes critical with more stringent carbon emission constraints, as wind and solar cannot cost-effectively provide reliable power due to their intermittency and high cost of electricity storage.

On the other side, the unique role of TES to integrate high shares of intermittent renewables in power generation, industry and buildings has been recognised in several studies such as [24], which predicted that the TES sector would see its size triple by 2030. TES solutions are suggested to be particularly promising for mid- to long-duration storage applications, including seasonal storage, for sector coupling (integration of district heating/cooling and power systems) and for alleviating grid reinforcement.

The economics of coupling nuclear reactors with TES systems were investigated in several previous studies. Carlson et al. [25] evaluated the profitability of operating such combination (with and without secondary generators) in deregulated US electricity grid. The study concluded that adding TES systems and secondary generators to nuclear reactors increases the total revenues by 3–8 % and the internal rate of return (IRR) by 25–35 %. Furthermore, Borowiec et al. [26] investigated the potential economic benefits of operating a large nuclear reactor integrated with a TES system in five US electricity markets. The study considered different penetrations of solar and wind power at various investment costs. The study concluded that such integration could be profitable, but it is highly reliant on: (i) the installed capacity of nuclear, solar and wind power in the grid, (ii) the shares of solar and wind power; (iii) the electricity market regulations in place; and (iv) the capital costs of the TES system.

The economic feasibility of integrating the UK's current fleet of advanced gas-cooled reactors (AGRs) with PCM-based TES systems and secondary organic Rankine cycle (ORC) generators was investigated by Romanos et al. [27]. In the study, different integration options based on technical constraints were proposed and the results showed that the peak power output could be increased by 24 % (from 670 to 822 MW_{el}) when the stored thermal energy is discharged using secondary ORC generators. The study concluded that the economics of upgrading nuclear power plants is highly dependent on: (i) the size of the secondary ORC generators; (ii) the price difference between the average peak and off-peak electricity prices; and (iii) the duration and frequency of TES charging/discharging cycles. The economic benefits of integrating nuclear with energy storage are not limited to the nuclear side but can also materialise at the energy storage side. For example, Park et al. [28] compared the thermodynamics and the economics of nuclear-integrated liquid air energy storage systems (LAES). The results showed that this coupling reduces the LCOE of a standalone LAES by 17 % (i.e., from $220/$MWh_{el}$ to $183/$MWh_{el}$). Additionally, this integration resulted in increasing the capacity factor of the nuclear power plant by 3 % due to the ability of storing generated heat. All of these studies demonstrated the possibility of generating profits through the integration on nuclear units with TES systems and secondary generation; however, the benefits for the overall electricity system have not been adequately investigated and quantified.

Previous study conducted by the authors [29] proposed a flexible configuration of nuclear power plant consisting of: a European pressurised reactor (EPR), a primary steam Rankine cycle (PSRC) system, and modular units consisting of TES and secondary steam Rankine cycle (SSRC) systems. The modular TES-SSRC units were designed to contain four phase change material (PCM) tanks and two SSRC systems. The study included: i) optimisation of the thermodynamic parameters of the system to maximise cycle efficiency; ii) preliminary design and material selection of PCM tanks; iii) design and thermodynamic parameters optimisation of SSRC; iv) development of power system model that minimises the total investment and operation costs with and without flexible nuclear power plants; and v) quantification of system benefits (i.e., cost savings) offered by added nuclear flexibility across a range of system scenarios with decarbonised electricity supply and high shares of renewables.

The results of Ref. [29] showed that the two designed SSRC systems could operate with cycle efficiencies of 30 % and 24 %, depending on the temperature range of the TES systems. It was also found that replacing conventional with flexible nuclear power plants could result in whole-system cost savings between £24 m/yr and £89 m/yr, depending on the selected low-carbon system scenario. Furthermore, the study estimated the cost of added flexibility (i.e., the cost of SSRC and TES systems) at £42.7 m/yr, which makes the proposed flexibility upgrades to the nuclear power plants economically justified in most of the plausible system decarbonisation scenarios. However, the analysis proposed in Ref. [29] assumed fixed sizes of TES and SSRC systems coupled to the existing nuclear power plants to achieve operational flexibility.

The aim of this paper is to expand the previous analysis from Ref. [29] by enhancing the high-resolution system optimisation model to be able to cost-optimise the sizes of different components of flexible nuclear plants concurrently with optimising investments in other assets in the energy system. This will allow for identifying cost-efficient system-driven configurations of nuclear plants instead of assuming fixed component sizes (i.e., a pre-defined configuration as used in Ref. [29]). This represents a key novelty in the system-led design of flexible nuclear technology, which to the authors' knowledge has not been addressed in the literature so far.

More specifically, the key contributions of this paper include: i) development of a novel energy system model that is able to co-optimise investment and operation in electricity and hydrogen production and storage assets as well as optimise the investment in flexible nuclear plant components, ii) development of reliable cost estimates for flexible nuclear plant components based on extensive survey of recent literature; and iii) carrying out a range of case studies for two archetypal systems (North and South) and a wide range of system scenarios to investigate how system features affect cost-optimal choices for flexible nuclear plant configurations.

2. Methods

This section presents the layout for upgrading a conventional nuclear power plant with a TES system and secondary power generation cycles. This is followed by the formulation of a detailed electricity system model developed in order to determine cost-efficient designs of flexible nuclear plant in order to minimise overall system cost in a low-carbon electricity system.

2.1. Power plant configuration and description

The assumed layout of a flexible nuclear power plant is shown in Fig. 1, which consists of:

(1) Nuclear power island with a European pressurised reactor (EPR) and a steam generator (SG);
(2) Primary steam Rankine cycle (PSRC) system that is directly connected to the SG;
(3) Two TES systems (TES-1 and TES-2), each consisting of two PCM tanks that are connected in series (system TES-1 includes PCM-1 and PCM-2 tanks and system TES-2 consists of PCM-3 and PCM-4 tanks); and
(4) Two secondary power generation cycle systems (SSRC-1 and SSRC-2). System SSRC-1 is operated by thermal energy stored in system TES-1 while system SSRC-2 is operated by utilising the heat stored in system TES-2.

The main operating conditions of the EPR, SG, PSRC, SSRC, and TES systems are listed in Table 1. Other thermodynamic parameters of the PSRC and the SSRCs, the material selection for the PCM tanks and the thermodynamic model explanation and set up can be found in Ref. [29].

Table 1
Key thermodynamic parameters of the considered flexible nuclear power plant [29].

Parameter	Value
European pressurised reactor thermal power (MW_{th})	4520
Steam generator outlet temperature (°C)	293
Steam generator outlet pressure (kPa)	7800
PSRC maximum electrical power output (MW_{el})	1610
PSRC thermal efficiency (%)	35.7
SSRC-1 thermal efficiency (%)	29.6
SSRC-2 thermal efficiency (%)	23.7
TES-1 charging steam temperature (°C)	293
TES-1 charging steam pressure (kPa)	7800
TES-2 charging steam temperature (°C)	221
TES-2 charging steam pressure (kPa)	2390

In typical operating conditions, the EPR and the SG would aim to continuously operate at full output in order to maximise their economic returns and take advantage of low fuel cost. However, during off-peak demand periods the PSRC system could operate at less than full-rated power output of 1610 MW_{el}, and the excess heat from the reactor could be stored in the attached TES systems. The stored heat can then be discharged to operate the SSRC systems during periods of high demand.

2.2. Whole-energy system modelling with flexible nuclear investment decisions

Investment decisions for various components of flexible nuclear plants have been integrated into a whole-energy system investment model presented in [30] and further modified in [29], in order to allow for identifying cost-efficient configurations of flexible nuclear plants. This paper builds on the previously developed WeSIM modelling framework that captures the interactions across various timescales and across various asset types at high temporal granularity, which is critical for studying low-carbon energy systems with high shares of variable renewable generation [30]. This framework allows for quantifying cost-efficient portfolios of different flexibility options, such as demand-side

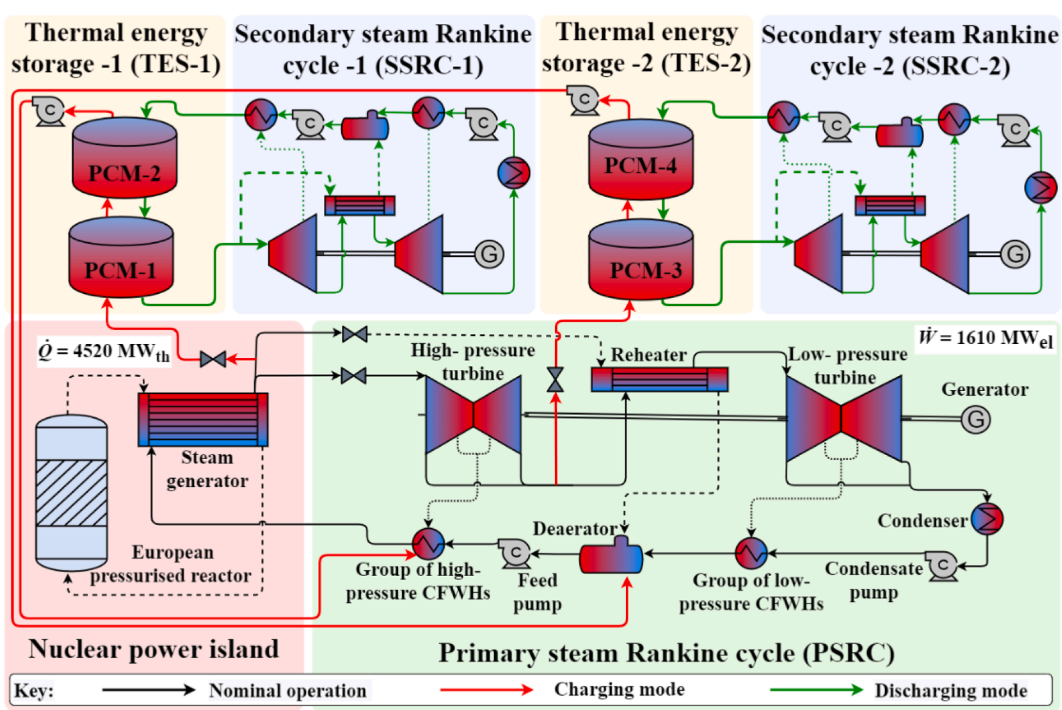

Fig. 1. Simplified schematics of the proposed flexible nuclear plant layout, which consists of conventional nuclear power plant (nuclear power island and PSRC system) and modular TES-SSRC units (SSRC-1, SSRC-2, TES-1 and TES-2 systems). Detailed layout with all cycle components can be found in Ref. [29].

response (DSR), energy storage or flexible generation technologies. The whole-system modelling approach has previously been applied to assess system benefits of various storage technologies, including battery storage [31], pumped-hydro [32] and liquid–air and pumped-heat energy storage [33]. The system optimisation model presented here has been implemented in FICO Xpress Optimisation framework [34].

The main inputs and outputs of the system optimisation model are illustrated in Fig. 2, which also includes the information received from the thermodynamic nuclear plant model described in the previous section. This information refers to the thermodynamic performance parameters of flexible nuclear plant components, including part-load and full-load efficiency of PSRC and SSRC generators, and charging and discharging efficiencies of PCM-based TES. Other inputs into the system model include the investment cost assumptions for electricity generation and storage assets and hydrogen production and storage assets, hourly profiles for electricity and hydrogen demand, fuel cost assumptions and system-level carbon constraints. Key outputs from the model include the investment decisions for production and storage assets as well as their hourly operation. These decisions also include the decisions for cost-optimal investment in flexible nuclear plant components, which also allows for quantifying their net system benefits.

2.3. Mathematical formulation of the whole-system model

The formulation of the system model presented here assumes a single-node system without considering any distribution, transmission or interconnection assets. A shortened form of the objective function for the mixed-integer linear problem is given in Equations (1)-(4). The model minimises the total system cost, which is the sum of annualised investment and operation cost associated with power generation and battery energy storage systems (BESS) (Equation (2)), flexible nuclear plants (Equation (3)) and hydrogen supply and storage (Equation (4)). The annual operating cost is quantified across all 8760 h of a year.

The objective function consists of three main terms: electricity system cost, cost of flexible nuclear plant and the cost of hydrogen supply system:

$$\min z = \varphi_{\mathrm{el}} + \varphi_{\mathrm{fn}} + \varphi_{\mathrm{H2}} \tag{1}$$

$$\varphi_{\mathrm{el}} = \sum_{g=1}^{G} \pi_g^{\mathrm{gen}} \mu_g^{\mathrm{gen}} + \sum_{s=1}^{S} \pi_s^{\mathrm{bs}} \mu_s^{\mathrm{bs}} + \sum_{t=1}^{T} \sum_{g=1}^{G} c_{g,t}^{\mathrm{gen}} \tag{2}$$

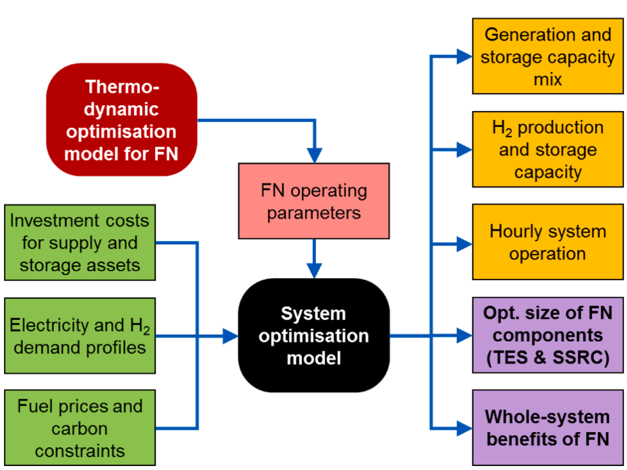

Fig. 2. Flowchart of the main inputs and outputs from the thermodynamic plant model and system optimisation model (FN = flexible nuclear).

$$\varphi_{\mathrm{fn}} = \sum_{f=1}^{F} \left(\pi_{\mathrm{PSRC},f}^{\mathrm{fn}} \mu_{\mathrm{PSRC},f}^{\mathrm{fn}} + \pi_{\mathrm{SSRC},f}^{\mathrm{fn}} \mu_{\mathrm{SSRC},f}^{\mathrm{fn}} + \pi_{\mathrm{TES},f}^{\mathrm{fn}} \mu_{\mathrm{TES},f}^{\mathrm{fn}} + \pi_{\mathrm{SG},f}^{\mathrm{fn}} \mu_{\mathrm{SG},f}^{\mathrm{fn}} \right) + \sum_{t=1}^{T} \times \sum_{f=1}^{F} Y_f^{\mathrm{fn}} h_{\mathrm{SG},f,t}^{\mathrm{fn}} \tag{3}$$

$$\begin{aligned} \varphi_{\mathrm{H2}} = & \sum_{e=1}^{E} \pi_e^{\mathrm{elH2}} \mu_e^{\mathrm{elH2}} + \sum_{r=1}^{R} \pi_r^{\mathrm{ref}} \mu_r^{\mathrm{ref}} + \sum_{u=1}^{U} \pi_u^{\mathrm{hs}} \mu_u^{\mathrm{hs}} \\ & + \sum_{t=1}^{T} \left[\sum_{i=1}^{I} F_i^{\mathrm{imp}} \xi_{i,t}^{\mathrm{imp}} + \sum_{e=1}^{E} A_e^{\mathrm{elH2}} \xi_{e,t}^{\mathrm{elH2}} + \sum_{r=1}^{R} \left(A_r^{\mathrm{ref}} + Y_{\mathrm{gas}} L_r^{\mathrm{gas}} \right) \xi_{r,t}^{\mathrm{ref}} \right] \end{aligned} \tag{4}$$

Component investment costs are expressed as products of per-unit cost parameters, π, and decision variables for total capacity, μ. The generation operating cost term, c^{gen}, is the function of generation output decision variables, p, and reflects the variable operating costs, no-load costs and start-up costs of thermal generators. Hydrogen system cost include the investment cost of electrolysers, reformers and hydrogen storage, as well as their operating costs, which also include the cost of gas for methane reformer operation.

2.3.1. Energy balance constraints

Power balance constraint ensures that the net output of all generation and BESS resources meets the electricity demand for each time interval, t, across all demand segments, while also supplying power to methane reformers and electrolysers:

$$\begin{aligned} & \sum_{g=1}^{G} p_{g,t}^{\mathrm{gen}} + \sum_{f=1}^{F} p_{f,t}^{\mathrm{fn}} + \sum_{s=1}^{S} \left(p_{\mathrm{dch},s,t}^{\mathrm{bs}} - p_{\mathrm{ch},s,t}^{\mathrm{bs}} \right) \\ & = \sum_{k=1}^{K} d_{k,t}^{\mathrm{el}} + \sum\nolimits_{r=1}^{R} L_r^{\mathrm{el}} \xi_{r,t}^{\mathrm{ref}} + \sum\nolimits_{e=1}^{E} L_e^{\mathrm{el}} \xi_{e,t}^{\mathrm{elH2}} \end{aligned} \tag{5}$$

Different demand segments are considered in the model and indexed by k (e.g., associated with baseline, appliance, heating and EV demand). The effect of DSR decisions is accounted for using demand shifting variables, δ, for each segment:

$$d_{k,t}^{\mathrm{el}} = D_{k,t}^{\mathrm{el}} + \delta_{k,t}^{\mathrm{el}+} + \delta_{k,t}^{\mathrm{el}-} \tag{6}$$

Volume of shifted demand for any segment and for any t is limited to a pre-specified fraction, γ, of the original demand, while the total volume of demand shifted away from original times needs to be compensated by increase in demand in other times of the day, adjusted for efficiency losses quantified through parameter, ψ:

$$\delta_{k,t}^{\mathrm{el}-} \le \gamma_k^{\mathrm{el}} D_{k,t}^{\mathrm{el}} \tag{7}$$

$$\sum_{t \in T_{\mathrm{day}}} \delta_{k,t}^{\mathrm{el}-} \le \psi_k^{\mathrm{el}} \sum_{t \in T_{\mathrm{day}}} \delta_{k,t}^{\mathrm{el}+} \tag{8}$$

Hydrogen balance equation ensures that total output of hydrogen from production technologies meets the total hydrogen demand, which consists of the external hydrogen demand (e.g., for industry or transport, net utilisation of hydrogen storage and the use of hydrogen for power generation:

$$\sum_{r=1}^{R} \xi_{r,t}^{ref} + \sum_{e=1}^{E} \xi_{e,t}^{elH2} + \sum_{i=1}^{I} \xi_{i,t}^{imp} = \sum_{u=1}^{U} \left(\xi_{ch,u,t}^{hs} - \xi_{dch,u,t}^{hs} \right) + \xi_t^{gen} + \Xi_t^{ext} \tag{9}$$

The volume of hydrogen used for power generation (i.e., to supply generators from subset HG) is quantified as follows:

$$\xi_t^{gen} = \sum_{\substack{g=1 \\ g \in HG}}^{G} \left(\alpha_g^{gen} n_{g,t}^{gen} + \beta_g^{gen} p_{g,t}^{gen}\right) \tag{10}$$

2.3.2. Constraints for thermal generators

Maximum new capacity for thermal generation technology g (belonging to the subset TG) is limited to a pre-specified upper bound, M_g^{new}:

$$\mu_g^{gen} \le M_g^{new} \forall g \in TG \tag{11}$$

Number of units of technology g in synchronised operation at time t is limited by the sum of existing capacity and the capacity added by the model:

$$n_{g,t}^{gen} P_g^{max} \le \mu_g^{gen} + M_g^{ex} \forall t \forall g \in TG \tag{12}$$

The allowed range for generator output level at time t is determined by the number of units in operation, n, and the minimum, P_g^{min}, and maximum, P_g^{max}, output for each unit:

$$n_{g,t}^{gen} P_g^{min} \le p_{g,t}^{gen} \le n_{g,t}^{gen} P_g^{max} \forall t \forall g \in TG \tag{13}$$

The operating cost of thermal generators is a function of its heat rates, α and β, and the cost of fuel, Y:

$$c_{g,t}^{gen} = \Delta\left(\alpha_g^{gen} n_{g,t}^{gen} + \beta_g^{gen} p_{g,t}^{gen}\right) Y_g^{gen} \forall t \forall g \in TG \tag{14}$$

The maximum annual output of generation technology g is limited based on the maximum annual utilisation factor, Ω:

$$\sum_{t=1}^{T} p_{g,t}^{gen} \le \left(\mu_g^{gen} + M_g^{ex}\right) P_g^{max} \Omega_g^{gen} T \forall g \in TG \tag{15}$$

Dynamic constraints for thermal generators related to ramping, start-up cost, provision of reserve, response and inertia and minimum up and down times have also been included in the model but are omitted here for brevity. Their detailed formulation can be found in [30].

2.3.3. Constraints for variable renewable generators

The capacity of variable renewable generators (belonging to subset RG) added by the model is limited to the pre-specified maximum capacity:

$$\mu_g^{gen} \le M_g^{new} \forall g \in RG \tag{16}$$

The sum of renewable output and curtailment is linked to the available capacity (new plus existing) and hourly availability, a, using the following relationship:

$$p_{g,t}^{gen} + w_{g,t}^{gen} = \left(\mu_g^{gen} + M_g^{ex}\right) a_{g,t}^{RES} \forall t \forall g \in RG \tag{17}$$

2.3.4. Constraints for battery storage

The maximum volume of new battery storage resource s is limited from above by M_s^{new}:

$$\mu_s^{bs} \le M_s^{new} \forall s \tag{18}$$

Charging and discharging rates of battery storage resources are limited by the installed capacity:

$$p_{dch,s,t}^{bs}, p_{ch,s,t}^{bs} \le \mu_s^{bs} \forall s \tag{19}$$

The energy balance of battery storage and the limit on its energy content (i.e., the state of charge) are formulated as follows:

$$q_{s,t}^{bs} = q_{s,t-1}^{bs} + \Delta\left(\eta_{ch,s}^{bs} p_{ch,s,t}^{bs} - \frac{1}{\eta_{dch,s}^{bs}} p_{dch,s,t}^{bs}\right) \tag{20}$$

$$q_{s,t}^{bs} \le \mu_s^{bs} \tau_s^{bs} \tag{21}$$

2.3.5. Constraints for hydrogen production and storage

Constraints on new capacity for electrolysers, reformers and hydrogen storage are formulated as follows:

$$\mu_e^{elH2} \le M_e^{new} \forall e \tag{22}$$

$$\mu_r^{ref} \le M_r^{new} \forall r \tag{23}$$

$$\mu_u^{hs} \le M_u^{new} \forall u \tag{24}$$

Constraints on output of hydrogen production and storage resources are linked to installed capacities:

$$\xi_{e,t}^{elH2} \le \mu_e^{elH2} \forall e \tag{25}$$

$$\xi_{r,t}^{ref} \le \mu_r^{ref} \forall r \tag{26}$$

$$\xi_{i,t}^{imp} \le M_i^{imp} \forall i \tag{27}$$

$$\xi_{ch,u,t}^{hs}, \xi_{dch,u,t}^{hs} \le \mu_u^{hs} \forall u \tag{28}$$

Hydrogen storage balance constraint and the upper limit on its energy content are formulated in the following way:

$$q_{u,t}^{hs} = q_{u,t-1}^{hs} + \Delta\left(\eta_{ch,u}^{hs} \xi_{ch,u,t}^{hs} - \frac{1}{\eta_{dch,u}^{hs}} \xi_{dch,u,t}^{hs}\right) \tag{29}$$

$$q_{u,t}^{hs} \le \mu_u^{hs} \tau_u^{hs} \tag{30}$$

2.3.6. Constraints for flexible nuclear generators

Investments in flexible nuclear components are subject to pre-specified limits:

$$\mu_{PSRC,f}^{fn} \le M_{PSRC,f}^{new}, \mu_{SSRC,f}^{fn} \le M_{SSRC,f}^{new}, \mu_{SG,f}^{fn} \le M_{SG,f}^{new}, \mu_{TES,f}^{fn} \le M_{TES,f}^{new} \tag{31}$$

Number of units in synchronised operation is bound by the total capacity added by the system:

$$n_{PSRC,f,t}^{fn} P_{PSRC,f}^{fn,max} \le \mu_{PSRC,f}^{fn}, n_{SSRC,f,t}^{fn} P_{SSRC,f}^{fn,max} \le \mu_{SSRC,f}^{fn} \tag{32}$$

Electricity output limits for PSRC and SSRC components are formulated as follows:

$$n_{PSRC,f,t}^{fn} P_{PSRC,f}^{fn,min} \le p_{PSRC,f,t}^{fn} \le n_{PSRC,f,t}^{fn} P_{PSRC,f}^{fn,max} \tag{33}$$

$$n_{SSRC,f,t}^{fn} P_{SSRC,f}^{fn,min} \le p_{SSRC,f,t}^{fn} \le n_{SSRC,f,t}^{fn} P_{SSRC,f}^{fn,max} \tag{34}$$

The aggregate electricity output of a flexible nuclear plant is equal to the sum of total PSRC and SSRC output:

$$p_{f,t}^{fn} = p_{PSRC,f,t}^{fn} + p_{SSRC,f,t}^{fn} \tag{35}$$

Charging and discharging of TES component of flexible nuclear units is limited by the installed TES capacity:

$$h_{f,t}^{TES,ch}, h_{f,t}^{TES,dch} \le \mu_{TES,f}^{fn} \tag{36}$$

TES energy balance equation at time t considers its state-of-charge (SOC) at the previous interval plus the effect of any charging or discharging activity adjusted for efficiency losses:

$$q_{TES,f,t}^{fn} = q_{TES,f,t-1}^{fn} + \Delta\left(\eta_{TES,Ch}^{fn} h_{f,t}^{TES,ch} - \frac{1}{\eta_{TES,Dch}^{fn}} h_{f,t}^{TES,dch}\right) \tag{37}$$

The limit on maximum energy stored in TES expressed via the product of its heat power and duration:

$$q_{TES,f,t}^{fn} \le \mu_{TES,f}^{fn} \tau_{TES,f}^{fn} \tag{38}$$

The SG heat output bounds are implemented as follows:

$$\omega_{SG,f}^{fn,min} \mu_{SG,f}^{fn} \le h_{SG,f,t}^{fn} \le \mu_{SG,f}^{fn} \tag{39}$$

Heat balance equations for the whole flexible nuclear plant take into account the output of SG, heat consumption of PSRC and SSRC generators and the charging and discharging decisions for TES:

$$h^{\text{fn}}_{\text{SG},f,t} - h^{\text{TES,ch}}_{f,t} = h^{\text{fn}}_{\text{PSRC},f,t} = \alpha^{\text{fn}}_{\text{PSRC},f} n^{\text{fn}}_{\text{PSRC},f,t} + \beta^{\text{fn}}_{\text{PSRC},f} p^{\text{fn}}_{\text{PSRC},f,t} \tag{40}$$

$$h^{\text{TES,dch}}_{f,t} = h^{\text{fn}}_{\text{SSRC},f,t} = \alpha^{\text{fn}}_{\text{SSRC},f} n^{\text{fn}}_{\text{SSRC},f,t} + \beta^{\text{fn}}_{\text{SSRC},f} p^{\text{fn}}_{\text{SSRC},f,t} \tag{41}$$

To reflect limited annual availability due to e.g., maintenance, a limit is imposed on total annual SG output:

$$\sum_{t=1}^{\tau} h^{\text{fn}}_{\text{SG},f,t} \le \mu^{\text{fn}}_{\text{SG},f} \Omega^{\text{fn}}_{\text{SG},f} T \tag{42}$$

2.3.7. System-wide carbon constraint

Total carbon emissions in the system result from the operation of thermal generators and methane reformers, and are constrained to a user-specified annual target value:

$$\Delta \sum_{t=1}^{T} \left(\sum_{\substack{g=1 \\ g \in TG}}^{G} \left(\alpha^{\text{gen}}_{g} n^{\text{gen}}_{g,t} + \beta^{\text{gen}}_{g} p^{\text{gen}}_{g,t} \right) \epsilon^{\text{gen}}_{g} + \sum_{r=1}^{R} L^{\text{gas}}_{r} \varsigma^{\text{ref}}_{r,t} \epsilon^{\text{ref}}_{r} \right) \le \Phi_{CO_2} \tag{43}$$

2.3.8. Calculating system benefits of flexible nuclear units

System value of flexible nuclear generation in this paper has been quantified as a *net system benefit* of repowering a standard nuclear unit with flexible components including TES and SSRC generation, while taking into account the investment cost required for installing the TES and SSRC components. To quantify these benefits, the whole-system model is run not just for scenarios that optimise flexible nuclear configurations, but also for cases where flexible nuclear components were not available for investment, which allowed to construct a series of *counterfactual* scenarios. Any reduction in total system cost between counterfactual and flexible nuclear runs is quantified as net system benefit of flexible nuclear, which also includes the installation cost of flexible nuclear components.

2.4. Scenarios used for quantifying cost-efficient configurations of flexible nuclear plants

Given that the primary purpose of the analysis is to determine system-driven cost-efficient configurations of flexible nuclear plants, a number of various system scenarios have been developed to study the key drivers for the system-driven design of flexible nuclear plants. Two generic geographic systems have been assumed, North and South, both sized to broadly match the size of the UK electricity system with an annual demand of 400 TWh_{el}, but differing in the following key features:

(1) North system is characterised by colder climate conditions, which is reflected in about 5 times higher heating demand than in the South system. At the same time, the electricity demand for cooling is several times higher in the South (40 TWh_{el}) than in the North (6 TWh_{el}).
(2) The potential of Renewable Energy Sources (RES) is assumed to differ between the two systems so that the available wind utilisation factors in the North were much higher than in the South, while for solar photovoltaic (PV) generation the utilisation factor is assumed to be lower in North than in the South.

Due to their characteristics, these two archetypal systems can be mapped to many countries in Europe and beyond, implying that the results presented in this paper would apply more generally than just for a single electricity system. Key differences between the two systems are detailed in Table 2.

In all scenarios it was assumed that there is one nuclear unit on the system, with the PSRC rating of 1610 MW_{el}. The only exception to this was the scenario that assumed 5 such units were present in the system. In counterfactual scenarios this unit was assumed to have a conventional configuration with just the SG and PSRC. In flexible nuclear scenarios the model was allowed to add SSRC and TES capacity to the nuclear unit (or units) at a given cost, if this is cost-efficient (i.e., if it leads to lower total system cost). In all scenarios the capacity of the conventional nuclear units (i.e., without TES and SSRC) was kept fixed and was not optimised by the model, while all other generation and storage technologies were subject to optimisation.

Assumptions on investment costs of electricity generation technologies were based on the UK Government's projections of electricity generation costs [35]. Similarly, cost assumptions and technical parameters for hydrogen production technologies were aligned with the UK Government's hydrogen production cost projections [36].

A range of scenarios is investigated for each of the two systems (North and South), as specified in Table 3. The aim of specifying these scenarios is to investigate the impact of various system features and assumptions on cost-efficient system-driven design of flexible nuclear plants. System features included in the scope of the analysis include the system carbon emission target, number of nuclear units in the system, higher interest rate, cost of battery storage, and the availability of investment into carbon offsets through Bioenergy with Carbon Capture and Storage (BECCS).

Table 2
Key features of North and South electricity systems.

Parameter	North	South
Electrified heating demand	High	Low
Cooling demand	Low	High
Onshore wind capacity factor	36 %	35 %
Offshore wind capacity factor	58 %	49 %
Solar PV capacity factor	14 %	24 %

2.5. Cost assumptions for flexible nuclear plant components

Specific investment costs of the SSRC and TES systems (PCM tanks) are estimated based on the information available in the relevant literature, as listed in Table 4. The SSRC system costs are obtained from steam Rankine cycle-based power generation blocks with similar sizes and similar technical properties. The reported costs of PCM tanks refer to similar PCM tank designs (i.e., with a shell and tubes) and with similar temperature limits.

The average of the specific investment cost of SSRC systems is £702/kW_{el} and the maximum relative difference between the reported costs is 17 %. This suggests that using the average specific investment cost is an acceptable assumption. Furthermore, the average specific investment cost of the PCM tanks is £15.9/kWh_{th} with a standard deviation of £1.6/kWh_{th}, which also suggests the average value is a reasonable estimate. Note that the assumed GBP/USD and GBP/EUR exchange rates were 0.80 and 0.85, respectively, based on Ref. [37].

Table 3
List of system scenarios used for studying cost-efficient configurations of flexible nuclear plants.

No.	Scenario description
1	Net zero carbon system
2	Carbon intensity target of 25 gCO_2/kWh
3	Carbon intensity target of 50 gCO_2/kWh
4	5 nuclear units instead of one
5	High interest rate (IR) of 8.9 % instead of 5 %
6	Higher cost of battery storage (50 % higher than baseline)
7	No investment in carbon offsets (BECCS)

Table 4
Specific investment costs of SSRC systems and PCM tanks.

Component	Cost 1	Cost 2	Cost 3	Average	Standard deviation
SSRC systems (£/kW$_{el}$)	643 [38]	748 [39]	715 [40]	702	43.9
PCM tanks (£/kWh$_{th}$)	14.6 [41]	15.4 [42]	17.7 [43]	15.9	1.6

3. Results and discussion

This section presents the results of the modelling runs that optimised the configuration of flexible nuclear plant across a wide range of system scenarios. Key results include: (i) the configuration of the flexible nuclear plant, i.e., the sizing of SSRC and TES components for a given size of SG and PSRC components; (ii) system cost savings resulting from cost-optimal flexible nuclear configurations; and (iii) illustrative hourly operation of the components of flexible nuclear plant.

3.1. Counterfactual system scenarios

In counterfactual scenarios for the North and South systems the generation and storage portfolios have been cost-optimised without the presence of flexible nuclear plants. The number of conventional nuclear units was always fixed at one except in the "5 units" scenario, when it was fixed at five units. Unlike other technologies, the capacity of conventional nuclear units was not optimised. The capacity mix obtained for these counterfactual scenarios is shown in Fig. 3.

In the North system wind represents the dominant generation technology, as the achievable annual utilisation factors are much higher than in the South, resulting in a lower LCOE. Generation portfolio in the South, on the other hand, is dominated by solar PV generation, driven by its higher capacity factor compared to the North system. In order to mitigate the variability in wind and PV output, in all scenarios there is a significant volume of battery storage (BESS), in the range of 62–95 GW in the North and 63–159 GW in the South. In addition to RES generation, all scenarios except "No BECCS" feature a considerable amount of unabated gas generation, namely Combined Cycle Gas Turbine (CCGT) and Open Cycle Gas Turbine (OCGT); its carbon footprint is mitigated by a relatively small amount of BECCS generation that delivers negative carbon emissions in order to deliver a given carbon target. In the Net zero scenario the required BECCS capacity is 4.6–5.9 GW, which reduces in less stringent emission scenarios (25 and 50 g/kWh).

In the No BECCS scenario the model was not allowed to invest in carbon offsetting BECCS technology, which effectively also prevented any unabated gas generation as part of the generation mix. As a result, the electricity demand is met by an increased amount of RES generation, supplemented by 21–25 GW of biomass generation and 9–14 GW of hydrogen generation (note that the volume of nuclear generation was fixed so the model could not add any further nuclear capacity). Although not depicted in Fig. 3, it is worth noting that in addition to investing in hydrogen generation capacity in the "No BECCS" scenarios, the model also invested in about 730 GWh of hydrogen storage and 14–15 GW$_{el}$ of electrolyser capacity, which was significantly higher than in other counterfactual scenarios.

Fig. 4 shows the breakdown of annual electricity supply across technologies across all counterfactual scenarios used in the study. Given that baseload low-carbon generation technologies such as nuclear and BECCS operate at relatively high annual capacity factors close to 90 % (unlike RES generation), their contribution in annual electricity supply is more pronounced than their contribution to the capacity portfolio in Fig. 3. The contribution of battery storage in annual electricity supply is shown as negative quantity that represents the difference between total annual discharging and total annual charging, where the latter is greater due to roundtrip efficiency losses. Note that because the use of hydrogen generation in the "No BECCS" scenarios also required the production of hydrogen from electrolysis, this resulted in increased demand for electricity compared to other scenarios, in order to supply the additional electrolyser demand.

3.2. Cost-efficient configurations of flexible nuclear plants

In each of the counterfactual scenarios the model was then allowed to add cost-optimal volumes of flexible components of nuclear plants (i.e., SSRC and TES capacity). All studies assumed a constant capacity of SG and PSRC components. The least-cost configurations of nuclear plants for various scenarios for the North and South systems are presented in Fig. 5, with the exception of the "No BECCS" scenario, the

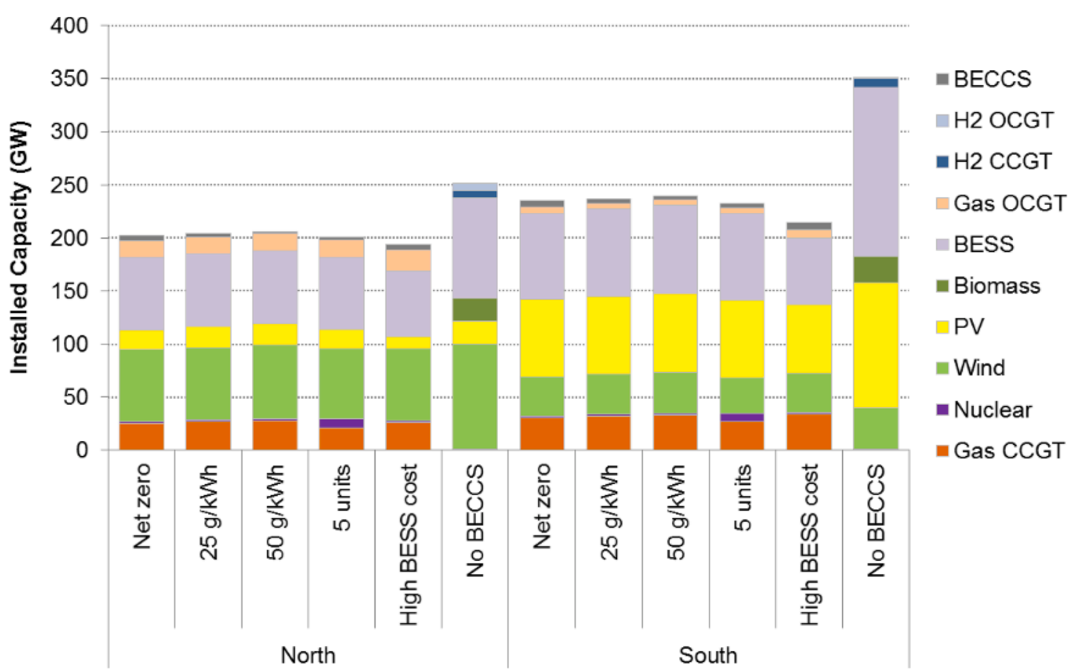

Fig. 3. Installed electricity generation and battery storage (BESS) capacity across various scenarios for North and South systems.

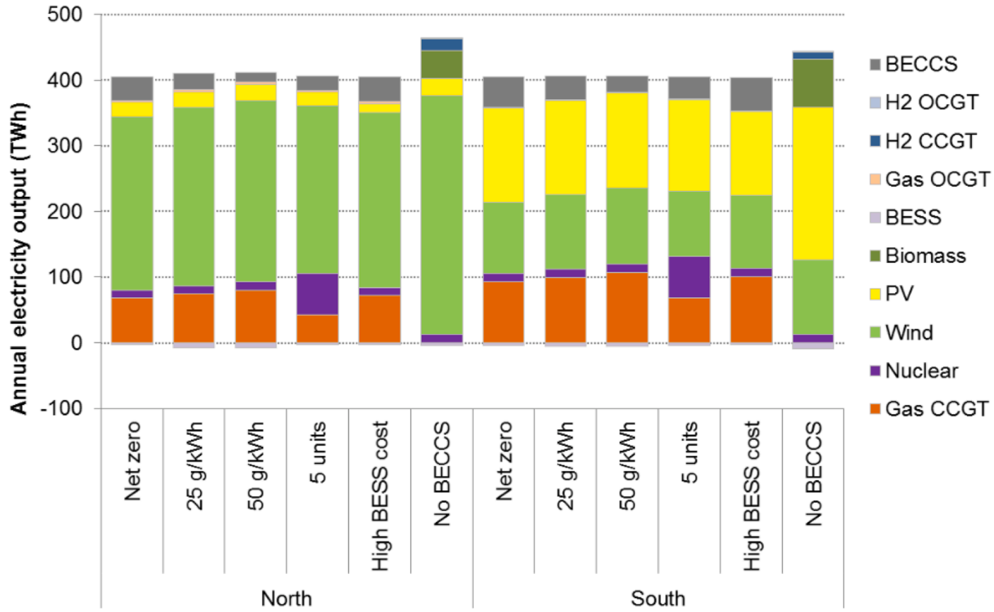

Fig. 4. Annual electricity output across various scenarios for North and South systems.

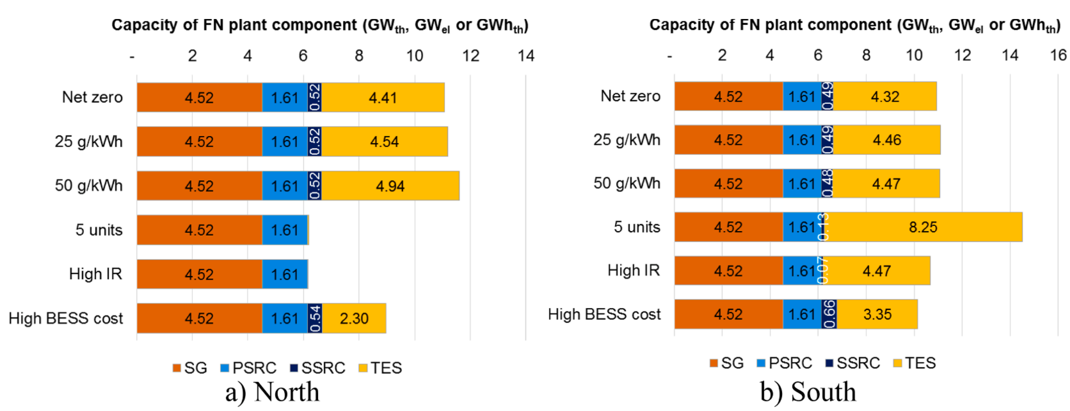

Fig. 5. Cost-optimal configurations of flexible nuclear plants across various scenarios for North and South systems. SG and PSRC sizes are kept constant for all scenarios and SSRC and TES sizes are optimised.

results of which are presented separately due to large differences in scale. Note that the sizes of different components in Fig. 5 are presented using different units although they have been plotted on the same chart: GW_{th} for SG, GW_{el} for PSRC and SSRC, and GWh_{th} for TES. Also note that the capacities have been expressed per one nuclear unit, so that in cases with 5 units any added SSRC and TES capacity has been divided by 5.

In the first three scenarios (Net zero, 25 g/kWh and 50 g/kWh) the model adds very similar amounts of SSRC capacity: 520 MW_{el} in the North system and 480–490 MW_{el} in the South system. These values are very close to the SSRC capacity of the pre-configured flexible nuclear plant assumed in Ref. [29]. The size of TES added by the model in the first three scenarios is 4.4–4.9 GWh_{th} in the North and 4.3–4.5 GWh_{th} in the South system, with slightly higher values observed in scenarios with less restricting emission targets. When these values are divided by the SSRC size and adjusted for SSRC electric conversion efficiency (26.3 %), the duration of TES in terms of hours of SSRC operation is found to be broadly between 2.2 and 2.5 h. This is considerably higher than the 1-hour duration previously assumed in Ref. [29].

In the North system scenarios with 5 units and High IR the model does not choose to add any flexibility to nuclear units as part of the cost-optimal solution. The benefits of flexibility offered by battery storage are higher in those scenarios then the benefits of enhancing the flexibility of nuclear plants. In the High IR scenario this occurs because of higher annual cost of enabling nuclear flexibility driven by a higher interest rate, while in the scenario with 5 units the higher nuclear capacity reduces the output of unabated gas plants and therefore releases some of their capacity to provide flexibility more cost-effectively.

In contrast, the flexibility requirements in the South system are higher due to greater fluctuations in PV output, so in the South the model adds some SSRC and TES capacity even when 5 nuclear units are present on the system or with high interest rates. In these cases, the model adds less SSRC capacity per unit then in the first three scenarios (although note that in the 5 units scenario the 130 MW_{el} of additional SSRC capacity per unit means 650 MW_{el} of SSRC capacity added in total). At the same time the volume of TES added is still significant at 8.2 GWh_{th} in the “5 units” scenario and 4.5 GWh_{th} in the “High IR” scenario, resulting in both cases in a similar TES duration of around 17 h.

Finally, the high BESS cost slightly increases the SSRC capacity added by the model, to 540 MW_{el} in the North and 660 MW_{el} in the South, but on the other hand the added TES capacity reduces to 2.3 GWh_{th} (North) and 3.3 GWh_{th} (South). This can be explained by observing that the counterfactual scenario with high BESS cost features less battery storage, less PV generation and more gas generation, all of which result in lower requirements for flexibility. The resulting TES durations in these two scenarios are 1.1 h in the North and 1.3 h in the South.

The results for cost-optimal configurations of flexible nuclear plants for the two "No BECCS" scenarios are presented in a separate chart in Fig. 6 alongside the main Net zero scenarios.

As noted before, the "No BECCS" scenario features a significant volume of hydrogen production (electrolysis), storage and H_2-fuelled electricity generation, as well as substantially higher volumes of BESS compared to other scenarios. Therefore, when flexible nuclear components are offered as investment options to the cost minimisation model, the cost-optimal solution maximises the TES volume by reaching the highest allowed volume specified in the model (100 units of 1948 MWh_{th} each). This is because in this scenario the system cannot rely on relatively cheap controllable gas generation (as its carbon emissions cannot be offset through BECCS), but rather has to invest in longer-term energy storage in the form of hydrogen, while also significantly increasing BESS capacity.

Although dwarfed by the increase in TES capacity in Fig. 6, the sizes of SSRC also increase in the "No BECCS" scenarios, to 4.7 GW_{el} in the North system and 1.4 GW_{el} in the South system.

The option to build relatively low-cost energy storage in the form of TES as part of flexible nuclear plants, therefore represents a highly attractive proposition, so that TES displaces some of the long-term hydrogen storage. Additional modelling experiments without the limit on new TES units revealed that the unconstrained cost-optimal volume of TES would be 370 GWh_{th} (North) and 495 GWh_{th} (South), also accompanied by significantly higher SSRC capacities. However, such high TES capacities acting as large-scale energy reservoirs are likely to exceed the realistic space constraints of actual nuclear power plants. Hence, these results could be interpreted to mean that nuclear plants in these scenarios should maximise the amount of TES they install as part of delivering a flexible plant configuration.

3.3. System benefits of flexible nuclear configurations

Flexible nuclear components get chosen as investment options by the cost-optimising model because they can reduce the overall system cost compared to the counterfactual scenario. It is therefore of interest to quantify the magnitude of system cost reduction delivered through more flexible nuclear plant configurations. To that end, Fig. 7 quantifies changes in total system cost between relevant counterfactual scenarios and scenarios with the option to invest in flexible nuclear plants. System cost savings are broken down into key cost components (generation, operation, storage, electrolysis and H_2 storage) and contrasted against the cost of investing into flexible nuclear components in order to quantify net changes in total system cost. The "No BECCS" scenarios are

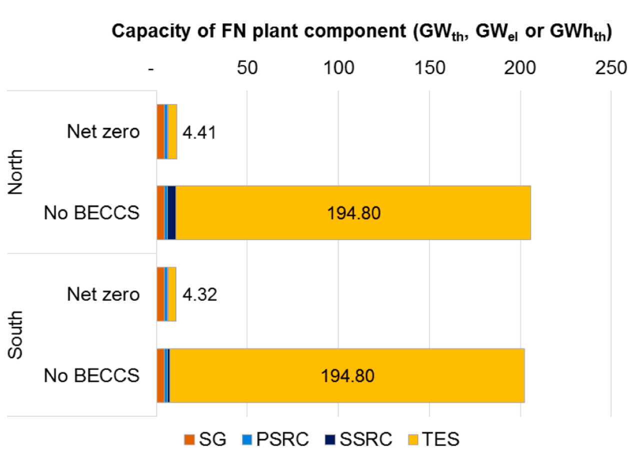

Fig. 6. Cost-optimal configurations of flexible nuclear plants for baseline Net zero and No BECCS scenarios for North and South systems.

again discussed separately due to differences in scale.

In the first three North system scenarios the net system benefits are in the range of £29-33 m/yr, which represents the difference between gross system benefits of £63-67 m/yr and the annualised investment cost into flexible nuclear components of around £34 m/yr. System cost savings are achieved predominantly by reducing the operating cost (OPEX) of BECCS and gas CCGT generators, reducing the investment cost of battery storage, while on the other hand investing slightly more in wind generation as the system with flexible nuclear is more capable of mitigating wind output fluctuations. Similar savings structure is observed in the South system for the first three scenarios, although the magnitude of total net savings is lower at around £19-20 m/yr.

In scenarios with 5 units and High IR the observed net system benefits are negligible in the North system as there is hardly any investment in flexible nuclear components, while in the South the respective net benefits are £11 m/yr and £2m/yr. Net system benefits in the "High BESS cost" scenarios are expectedly higher than the baseline Net zero scenarios, amounting to £46 m/yr in the North system and £27 m/yr in the South system.

Finally, in the "No BECCS" scenarios, which are not presented in Fig. 7, the maximisation of TES capacity results in even higher net system benefits: £266 m/yr in the North system and £94 m/yr in the South system. In these scenarios a significant proportion of system cost savings comes from TES displacing hydrogen storage and electrolyser investment.

To further illustrate how the addition of flexible nuclear components affects the cost-optimal generation and storage capacity mix, Fig. 8 shows the changes in the cost-optimal capacity portfolios observed when the model is allowed to invest in flexible nuclear components. The results are shown for both North and South systems. As with the system benefits presented in Fig. 7, these capacity differentials are calculated by comparing the capacities between various scenarios when flexible nuclear components are available for investment and the corresponding counterfactuals. Capacity changes for the "No BECCS" scenario in North and South systems are shown on a separate scale as the magnitude of changes in this scenario significantly exceeds the changes observed in other scenarios.

For the first three scenarios in the North system (Net zero, 25 g/kWh and 50 g/kWh) the addition of nuclear flexibility generally increases the volume of wind in the system, while reducing the volume of BESS as part of the cost-optimal portfolio. In the Net zero scenario the model also adds more PV capacity with flexible nuclear available in the system, while displacing some of the required carbon-negative BECCS generation and peaking OCGT capacity. As carbon constraints become less stringent, the model reduces solar PV capacity, i.e., replaces it with more cost-efficient wind generation in the North; at the same time, flexible nuclear displaces more gas CCGT generation and less BECCS and OCGT capacity.

Changes observed in the "High BESS cost" scenario are similar to those observed in the "Net zero" scenario, except that more BESS and gas CCGT capacity is displaced while the OCGT capacity increases as it represents a more cost-effective option for peaking capacity than high-cost BESS. Capacity changes in the "5 units" and "High IR" scenarios are negligible, as there is no investment in flexible nuclear components in those scenarios. Finally, in the "No BECCS scenario" the 4.7 GW of added flexible nuclear (i.e., SSRC) capacity displaces a significant volume of BESS (around 10.5 GW), as well as 2.4 GW of hydrogen CCGT and OCGT capacity.

In the South system a very similar effect on the capacity mix is observed for the first three scenarios. Additional power generation capacity offered by flexible nuclear units (about 0.5 GW) displaces a similar amount of BESS capacity, while at the same time allowing more wind and solar PV capacity to be added to the system. Additional wind and PV displace some of the output of gas CCGT and BECCS generation, as well as compensate for the reduced net output of nuclear (as added flexibility also means additional losses incurred when charging and

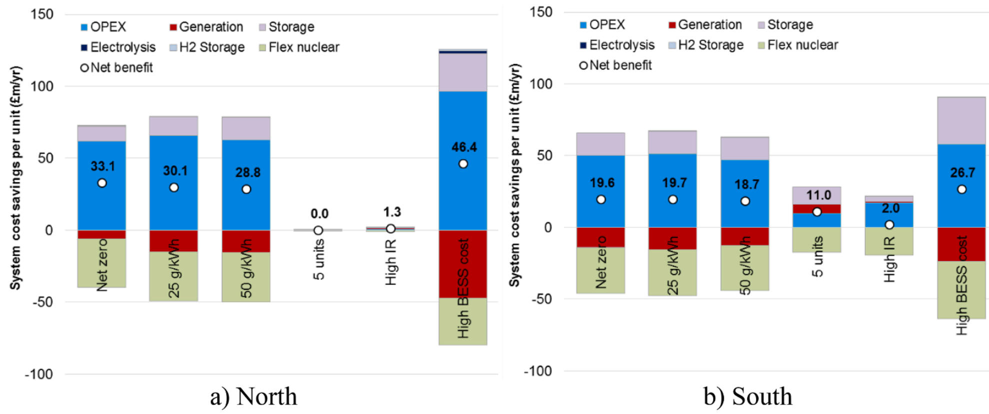

Fig. 7. System cost savings from flexible nuclear plants across various scenarios for North and South systems.

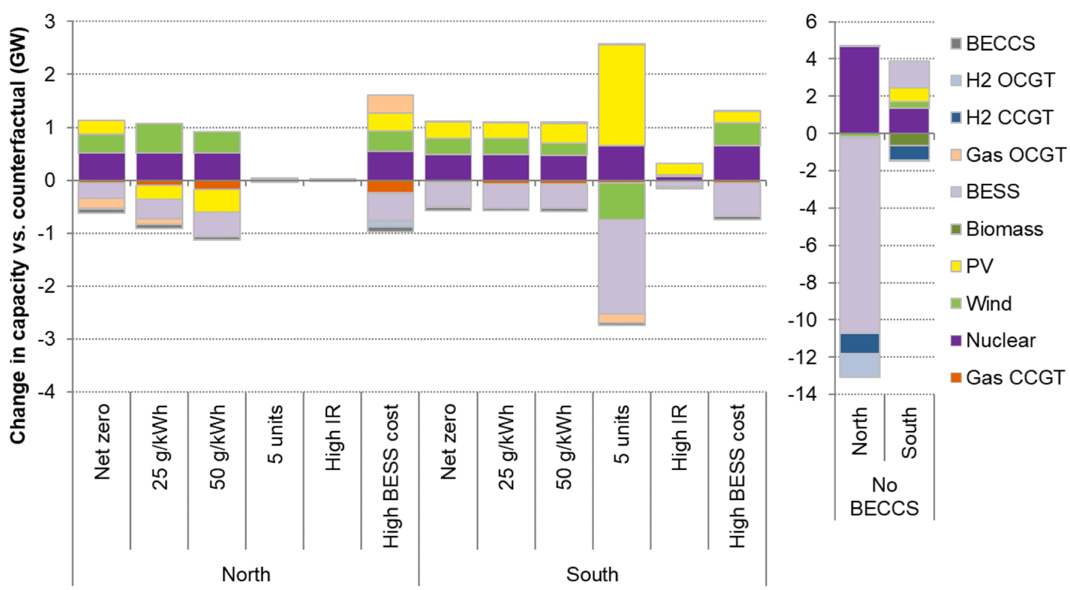

Fig. 8. Changes in cost-optimal capacity mix in scenarios with allowed investment in flexible nuclear plants measured against counterfactual scenarios.

discharging TES). A similar trend is also observed in the "High BESS cost" scenario, with capacity changes amplified by the higher cost of competing flexibility in the form of BESS.

In the "5 units" scenario the significantly higher volume of flexibility offered by nuclear units with TES and SSRC generation allows more of the low-cost solar PV resource to be integrated onto the system more efficiently, as nuclear output can better complement the daily variations of PV output; as a result, some of the wind capacity in this case gets replaced by solar PV. In the "High IR" scenario the impact on the capacity mix is marginal as the model does not choose to invest in any significant volume of flexible nuclear components. Finally, in the "No BECCS" case with a markedly different mix in the counterfactual scenario, flexible nuclear displaces the need for relatively costly biomass and hydrogen generation (as well as the associated capacity for hydrogen production and storage) and allows them to be replaced with cheaper wind and solar PV resources coupled with more BESS. One of the drivers for this effect is that TES in flexible nuclear effectively replaces some of the hydrogen storage that is used for long-term energy storage, which is essential in highly renewable systems with no carbon offsets.

3.4. Hourly operation of flexible nuclear components

Finally, in order to illustrate short-term operation of flexible nuclear components, two examples of hourly operation diagrams are provided for selected weeks for North and South systems.

Fig. 9 represents a winter week in the North system for the Net zero scenario. The chart shows hourly variations in SG heat output, power output of PSRC and SSRC, thermal input into and output from TES and the TES state-of-charge (SOC). To illustrate system drivers for the utilisation of flexible nuclear components, the chart also includes the net system demand profile, which is obtained by deducting wind and PV generation from system electricity demand.

The results suggest that TES and SSRC are used to generate electricity during periods of high net demand on Days 2 and 7 of the week shown in Fig. 9. On some occasions the TES is charged immediately after being discharged in order to be ready for the next peak (Day 2), while on others it charges gradually during periods of relatively lower net demand driven by higher wind output (Days 3–5) in order to be ready to discharge again when net demand increases. In general, there is no regular daily pattern of TES and SSRC utilisation, but rather a correlation with high and low wind output periods (resulting in low and high net system demand).

In the South system, on the other hand, as shown in Fig. 10, the operation of flexible nuclear components follows a fairly regular daily cycle. The week depicted in Fig. 10 is a summer week with significant contribution from solar PV generation, reflected in sharp dips in net system demand around the middle of each day. The optimal operating

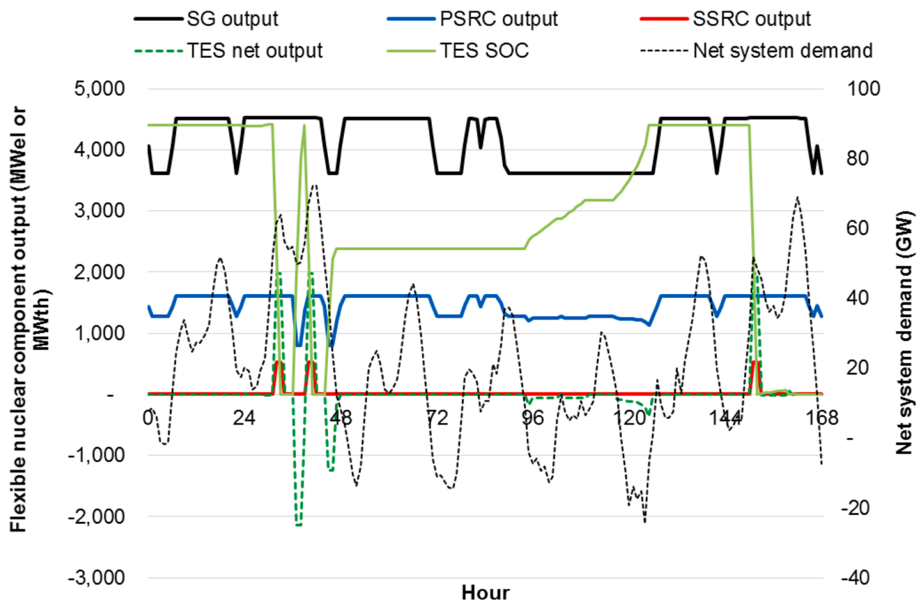

Fig. 9. Hourly operation of flexible nuclear generation during a winter week in the North system for the Net zero scenario. Net system demand represents the difference between system demand and total wind and PV output and is plotted against the right-hand axis.

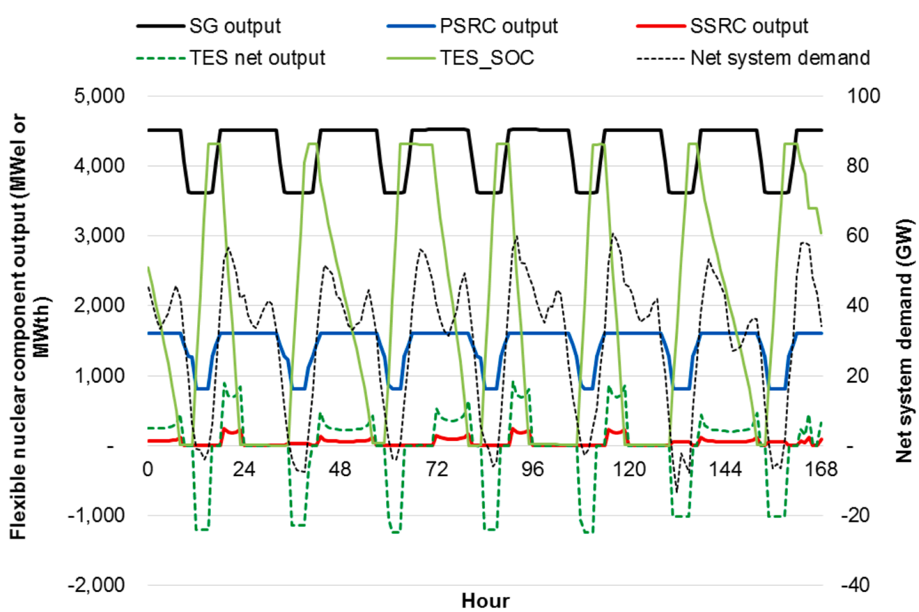

Fig. 10. Hourly operation of flexible nuclear generation during a summer week in the South system for the Net zero scenario. Net system demand represents the difference between system demand and total wind and PV output and is plotted against the right-hand axis.

strategy for flexible nuclear plant in this case is to minimise its PSRC output around midday and use excess heat from SG to charge TES. As net demand increases sharply in early evening hours, the PSRC output returns to is maximum level, supplemented by additional generation from SSRC to utilise the energy stored in TES during periods of high PV output. One can also observe that, unlike in the North system, TES gets fully charged and discharged every day.

4. Conclusions

This paper proposed a novel high-resolution system optimisation model that determines cost-optimal sizes of different components of flexible nuclear plants as part of cost optimisation of the wider energy system. This approach identifies cost-efficient system-driven configurations of nuclear plants as function of system characteristics, which represents a significant improvement with respect to previous approaches that assessed the benefit of flexible nuclear assuming a fixed plant configuration. Based on plausible cost estimates for flexible nuclear plant components derived from an extensive literature survey, a range of system scenarios have been analysed to study the impact of system features on cost-optimal choices for flexible nuclear plant configuration.

The results suggest that for a standard-size nuclear unit assumed in the paper, with the PSRC capacity of 1610 MW_{el}, it would be cost-efficient to install around 500 MW_{el} of SSRC capacity as well as around 4.5 GWh_{th} of TES capacity in most low-carbon and net-zero carbon systems considered in the study. This would result in an equivalent TES duration of 2.2 h, which is substantially higher than the 1-hour duration assumed in previous work [29]. Enhancing the nuclear plant flexibility was found to be less attractive when applied to a larger number of nuclear units or when exposed to high interest rates in the North system, which was characterised by high heating demand and by wind as the dominant renewable resource. On the other hand, in the South system dominated by PV generation and characterised by milder weather, flexible nuclear investment was attractive even in those scenarios.

High BESS cost was found to slightly increase the cost-optimal SSRC capacity, but on the other hand reduce the added TES capacity. Finally, in net-zero carbon scenarios without available carbon offsets (BECCS) the model maximised the TES volume in flexible nuclear suggesting its very high value for the net-zero systems. Nevertheless, such high TES capacities are not likely to be feasible due to space constraints.

Net system benefits per unit of flexible nuclear generation for the main net-zero and low-carbon scenarios were found to be in the range of £29-33 m/yr in the North and £19-20 m/yr in the South, suggesting a positive economic effect of investing in flexible nuclear plant components. Net benefits reduce in scenarios with 5 units and high interest rates but increase slightly with higher BESS cost. In scenarios without available BECCS carbon offsets the net benefits of flexible nuclear increase substantially, although this increase would be subject to constraints on the volume of TES that can be realistically added to a nuclear plant.

The approach to system-driven technology design presented in this paper can be extended to many other energy technologies. A recent example of system-led design of zero-carbon heating technologies is presented in [44].

Future work in this area will continue to study the thermodynamic properties of various flexible nuclear plant configurations to validate the feasibility of various system-driven configurations and refine the solution, while also establishing a feedback loop into the detailed thermodynamic design of plant components, including the number and type of SSRC and TES components. Future work will also focus on the use of integrated TES solutions to increase mid-to-long duration energy storage and systems flexibility [45], including electric reversible heat pumps [46,47], liquid air or compressed air solutions [48] or heat decarbonization solutions [49,50].

CRediT authorship contribution statement

Marko Aunedi: Conceptualization, Data curation, Formal analysis, Methodology, Software, Validation, Visualization, Writing – original draft, Writing – review & editing. **Abdullah A. Al Kindi:** Data curation, Formal analysis, Methodology, Software, Validation, Visualization, Writing – original draft, Writing – review & editing. **Antonio M. Pantaleo:** Conceptualization, Formal analysis, Methodology, Writing – review & editing. **Christos N. Markides:** Funding acquisition, Methodology, Project administration, Resources, Supervision. **Goran Strbac:** Conceptualization, Funding acquisition, Project administration, Resources, Supervision.

Declaration of Competing Interest

The authors declare that they have no known competing financial interests or personal relationships that could have appeared to influence the work reported in this paper.

Data availability

Data will be made available on request.

Acknowledgment

The research presented in this paper has been supported by the UK Engineering and Physical Sciences Research Council (EPSRC) [grant number EP/R045518/1] (IDLES Programme). A shorter version of this paper has been presented during the 17th Conference on Sustainable Development of Energy, Water and Environment Systems (SDEWES) held in Paphos, Cyprus, 6-10 November 2022.

References

[1] International Atomic Energy Agency (IAEA), Climate Change and Nuclear Power 2020, https://www.iaea.org/publications/14725/climate-change-and-nuclear-power-2020. [Accessed: 13-Jun-2022].
[2] Lazard's Levelized Cost of Energy Analysis – Version 15.0, October 2021, https://www.lazard.com/media/451905/lazards-levelized-cost-of-energy-version-150-vf.pdf [Accessed: 18-Jan-2023].
[3] World Nuclear Association, Nuclear Power in France, https://world-nuclear.org/information-library/country-profiles/countries-a-f/france.aspx. [Accessed: 10-Jan-2023].
[4] Campbell C. As Putin threatens nuclear disaster, Europe learns to embrace nuclear energy again, Time, 2022. https://time.com/6169164/ukraine-nuclear-energy-europe/ [Accessed: 13-May-2022].
[5] Department of Business, Energy & Industrial Strategy, Nuclear Industrial Strategy – The UK's Nuclear Future, 2013, https://www.gov.uk/government/publications/nuclear-industrial-strategy-the-uks-nuclear-future. [Accessed: 13-Jun-2022].
[6] Department of Business, Energy & Industrial Strategy, Climate Change Act 2008 (2050 Target Amendment) Order 2019, https://www.legislation.gov.uk/uksi/2019/1056. [Accessed: 13-Apr-2021].
[7] World Nuclear Association, Nuclear Power in the United Kingdom, https://world-nuclear.org/information-library/country-profiles/countries-t-z/united-kingdom.aspx. [Accessed: 10-Jan-2023].
[8] Strbac G, Pudjianto D, Aunedi M, Djapic P, et al., Role and value of flexibility in facilitating cost-effective energy system decarbonisation, *Progress in Energy*, 2, 2020.
[9] Aunedi M, Wills K, Green T, Strbac G. Net-zero GB electricity: cost-optimal generation and storage mix, Energy Futures Lab White Paper 2021, https://www.imperial.ac.uk/energy-futures-lab/reports/white-papers/net-zero-gb-electricity/ [Accessed 18-Jan-2023].
[10] Jenkins JD, Zhou Z, Ponciroli R, Vilim RB, Ganda F, de Sisternes F, et al. The benefits of nuclear flexibility in power system operations with renewable energy. Appl Energy 2018;222:872–84.
[11] Denholm P, King JC, Kutcher CF, Wilson PPH. Decarbonizing the electric sector: Combining renewable and nuclear energy using thermal storage. Energy Policy 2012;44:301–11.
[12] Curtis D, Shifflet N, Forsberg C. Technology Options for Integrated Thermal Energy Storage in Nuclear Power Plants. Trans Am Nucl Soc 2017;116:837–40.
[13] Carlson F, Davidson JH. On the use of thermal energy storage for flexible baseload power plants: Thermodynamic analysis of options for a nuclear Rankine cycle. J Heat Transfer 2020;142:052904.
[14] Carlson F, Davidson JH, Tran N, Stein A. Model of the Impact of Use of Thermal Energy Storage on Operation of a Nuclear Power Plant Rankine Cycle. Energ Conver Manage 2019;181:36–47.
[15] Carlson F, Davidson JH. Parametric Study of Thermodynamic and Cost Performance of Thermal Energy Storage Coupled With Nuclear Power. Energ Conver Manage 2021;236:114054.
[16] Li Y, Cao H, Wang S, Jin Y, et al. Load shifting of nuclear power plants using cryogenic energy storage technology. Appl Energy 2014;113:1710–6.
[17] Forsberg C. Hybrid systems to address seasonal mismatches between electricity production and demand in nuclear renewable electrical grids. Energy Policy 2013;62:333–41.
[18] Alameri SA. A coupled nuclear reactor thermal energy storage system for enhanced load following operation, Ph.D. Dissertation, Colorado School of Mines, Colorado, USA, 2015.
[19] Forsberg C, Brick S, Haratyk G. Coupling heat storage to nuclear reactors for variable electricity output with baseload reactor operation. Elect J 2018;31:23–31.
[20] Forsberg CW. Heat in a bottle. ASME Mech Eng 2019;141:36–41.
[21] Chae YJ, Lee JI. Thermodynamic analysis of compressed and liquid carbon dioxide energy storage system integrated with steam cycle for flexible operation of thermal power plant. Energ Conver Manage 2022;256:115374.
[22] Jiang K, Liu H, Li K. Amine-based thermal energy storage system towards industrial application. Energ Conver Manage 2023;283:116954.
[23] Duan L, Petroski R, Wood L, Caldeira K. Stylized least-cost analysis of flexible nuclear power in deeply decarbonized electricity systems considering wind and solar resources worldwide. Nat Energy 2022;7:260–9.
[24] International Renewable Energy Agency (IRENA), Innovation Outlook: Thermal Energy Storage, 2020, https://www.irena.org/publications/2020/Nov/Innovation-outlook-Thermal-energy-storage [Accessed: 18-Jan-2023].
[25] Carlson F, Davidson JH. Nuclear power coupled with thermal energy storage: impact of technical performance on economics in an exemplary electricity grid. ASME Open J Eng 2022;1:011006.
[26] Borowiec K, Wysocki A, Shaner S, Greenwood MS, Ellis M. Increasing revenues of nuclear power plants with thermal storage. J Energy Res Technol 2020;142:042006.
[27] Romanos P, Al Kindi AA, Pantaleo AM, Markides CN. Flexible nuclear plants with thermal energy storage and secondary power cycles: Virtual power plant integration in a UK energy system case study. e-Prime - Adv Elect Eng Electron Energy 2022;2:100027.
[28] Park JH, Heo JY, Lee JI. Techno-economic study of nuclear integrated liquid air energy storage system. Energ Conver Manage 2022;251:114937.

[29] Al Kindi AA, Aunedi M, Pantaleo AM, Strbac G, Markides CN. Thermo-economic assessment of flexible nuclear power plants in future low-carbon electricity systems: Role of thermal energy storage. Energ Conver Manage 2022;258:115484.
[30] Pudjianto D, Aunedi M, Djapic P, Strbac G. Whole-system assessment of value of energy storage in low-carbon electricity systems. IEEE Trans Smart Grid 2014;5(2):1098–109.
[31] Strbac G, Aunedi M, Konstantelos I, Moreira R, et al. Opportunities for energy storage: Assessing whole-system economic benefits of energy storage in future electricity systems. IEEE Power Energ Mag 2017;15:32–41.
[32] Teng F, Pudjianto D, Aunedi M, Strbac G. Assessment of future whole-system value of large-scale pumped storage plants in Europe. Energies 2018;11:246.
[33] Georgiou S, Aunedi M, Strbac G, Markides CN. On the value of liquid-air and pumped-thermal electricity storage systems in low-carbon electricity systems. Energy 2020;193:116680.
[34] FICO Xpress Optimization, https://www.fico.com/en/products/fico-xpress-optimization [Accessed: 13-Jun-2022].
[35] Department of Business, Energy and Industrial Strategy, Electricity generation costs, 2020, https://www.gov.uk/government/publications/beis-electricitygeneration-costs-2020 [Accessed 18-Jan-2023].
[36] Department of Business, Energy and Industrial Strategy, Hydrogen production costs, 2021, https://www.gov.uk/government/publications/hydrogenproduction-costs-2021 [Accessed 18-Jan-2023].
[37] Bank of England Database, Daily spot exchange rates against Sterling, https://www.bankofengland.co.uk/boeapps/database/Rates.asp?Travel=NIxAZx&into=GBP [Accessed: 21-May-2022].
[38] International Renewable Energy Agency (IRENA), Renewable power generation costs in 2020, 2021, Abu Dhabi, https://www.irena.org/-/media/Files/IRENA/Agency/Publication/2021/Jun/IRENA_Power_Generation_Costs_2020.pdf [Accessed: 27-Apr-2022].
[39] Black GA, Aydogan F, Koerner CL. Economic viability of light water small modular nuclear reactors: General methodology and vendor data. Renew Sustain Energy Rev 2019;103:248–58.
[40] Dersch J, Paucar J, Schuhbauer C, Schweitzer A, Stryk A. Blueprint for Molten Salt CSP Power Plant, Final report of the research project "CSP-Reference Power Plant" No. 0324253, 2021, Cologne, Germany. https://elib.dlr.de/141315/1/Blueprint%20for%20Molten%20Salt%20CSP%20Power%20Plant.pdf [Accessed: 27-Apr-2022].
[41] Bai F, Wang Y, Wang Z, Sun Y, Beath A. Economic evaluation of shell-and-tube latent heat thermal energy storage for concentrating solar power applications, *International Conference on Concentrating Solar Power and Chemical Energy Systems (SolarPACES) 2014*, *Energy Procedia*, vol. 69, pp. 737-747, 2015.
[42] Jacob R, Saman W, Belusko M, Bruno F. Techno-economic analysis of phase change material thermal energy storage systems in high temperature concentrated solar power plants. Asia-Pacific Solar Res Conference 2014.
[43] Jacob R, Belusko M, Fernandez AI, Cabeza LF, Saman W, Bruno F. Embodied energy and cost of high temperature thermal energy storage systems for use with concentrated solar power plants. Appl Energy 2016;180:586–97.
[44] Aunedi M, Olympios AV, Pantaleo AM, Markides CN, Strbac G. System-driven design of hybrid electricity- and hydrogen-based systems for domestic heat decarbonisation, *17th Conference on Sustainable Development of Energy, Water and Environment Systems (SDEWES)*, Paphos, Cyprus, 2022.
[45] McKinsey & Company, Net-zero power: Long duration energy storage for a renewable grid, 2021, https://www.mckinsey.com/capabilities/sustainability/our-insights/net-zero-power-long-duration-energy-storage-for-a-renewable-grid [Accessed 18-Jan-2023].
[46] Laughlin RB. Pumped thermal grid storage with heat exchange. J Renew Sustain Energy 2017;9:044103.
[47] Frate GF, Antonelli M, Desideri U. A novel Pumped Thermal Electricity Storage (PTES) system with thermal integration. Appl Therm Eng 2017;121:1051–8.
[48] Olympios AV, et al. Progress and prospects of thermo-mechanical energy storage—a critical review. Prog Energy 2021;3:022001.
[49] EnergyNest, Powering your clean energy transition, https://energy-nest.com/ [Accessed 18-Jan-2023].
[50] Kraftblock, Industrial energy storage system, https://kraftblock.com/en/ [Accessed 18-Jan-2023].